Transferring color between three-dimensional objects

Hui-Liang Shen and John H. Xin

A framework for transferring image-based color between three-dimensional objects by the use of a dichromatic reflection model is proposed. The framework addresses the following issues: (1) accurate recovery of an implicit geometric coefficient, (2) calculation of body color, (3) color transfer between different illuminants, and (4) segmentation of multicolored regions. The experimental results show that high color accuracy and photorealistic effects of the synthesized images can be achieved. The proposed technique has wide applications in image-based design and visualization of three-dimensional objects. © 2005 Optical Society of America

OCIS codes: 330.1690, 330.1720, 100.3020.

1. Introduction

Color is an important issue in the literature of computer graphics and image processing, including image rendering and enhancement. Reinhard *et al.* presented a method of transferring color to modify the perceptual appearance of a color image by use of simple statistical analysis in a decorrelated color space.[1] Based on the research reported in Ref. 1, Welsh *et al.* further proposed a method to colorize a gray-scale image by selecting swatches from another color image.[2] Most recently, Levin *et al.* presented a method for colorizing gray-scale image and video by the technique of seed-color propagation, according to the assumption that neighboring pixels with similar intensities should also have similar colors.[3] Although these methods performed well in the colorization of natural scenes, they did not deal with the color synthesis of three-dimensional (3-D) objects when highlights are present. In computer vision, a dichromatic reflection model was introduced by Shafer[4] and was used to model color reflection. Based on this model, Liu and Xu proposed modifying the color of an image scene and found that the model outperformed some baseline methods.[5] Most recently, Xin and Shen proposed a dichromatic-based color synthesis method that recovers the implicit geometric coefficient of a 3-D object's surface and investigated the color accuracy in both spectral reflectance and red–green–blue (RGB) spaces.[6]

Generally, to synthesize realistic images of 3-D objects accurately there should be a complete representation of the imaging geometry and reflection characteristics of object surfaces. For opaque surfaces, the bidirectional reflectance distribution function,[7] which is a function of the incident and the reflecting angles of light, is usually employed for color rendering. However, considering the limited accuracy of the apparatus for data collection and the difficulties in measurement of irregular surfaces,[8] it is desired to perform color rendering based on two-dimensional images.[6]

In this paper we propose an image-based color transfer method for modifying the colors of object surfaces in an image such that the color of the synthesized image appears perceptually close to that of the target image. More precisely, given two objects, I_1 and I_2, with different colors, the purpose is first to recover intrinsic color characteristics C_1 and C_2 from I_1 and I_2, respectively, and then to map C_2 onto object I_1 such that the color appearance of synthesized object I_1' is similar to that of I_2. This basic idea is close to that of our previous study.[6] In this paper we propose an integrated framework for color synthesis and transfer that includes the following components: First, the implicit geometric coefficient is calculated in a robust way by minimizing the propagation of error in color synthesis. Second, the colors of 3-D objects are reliably recovered by use of the high correlation among channels. Third, a new dichromatic-based segmentation algorithm is proposed for images that consist of multicolored regions. The proposed method can be applied to a variety of materials, such

H.-L. Shen (tcshenhl@polyu.edu.hk) and J. H. Xin (tcxinjh@inet.polyu.edu.hk) are with the Institute of Textiles and Clothing, The Hong Kong Polytechnic University, Hong Kong, China.

Received 20 April 2004; revised manuscript received 20 July 2004; accepted 25 August 2004.
0003-6935/05/101969-08$15.00/0

as plastics, ceramics, paper, and many textile fabrics, that can be described by the dichromatic reflection model. The proposed method is of potential use in the virtual design and visualization of 3-D objects, with the advantage of color accuracy. For example, this technique lets designers visualize the final color appearance of products before actual production and therefore improves their design efficiency.

2. Dichromatic-Based Modeling of Color Reflections

If we represent the spectral radiance of the illuminant by function $L(\lambda)$, with λ being the wavelength, and the spectral reflectance of the object surface at position p by $r^p(\lambda)$, the light entering the CCD camera then becomes $L(\lambda)r^p(\lambda)$. Let $S_k(\lambda)$ be the spectral sensitivity of the kth channel ($k = 1, 2, 3$) of the camera; the response of the camera becomes[9]

$$V_k^p = \int_\Omega L(\lambda)S_k(\lambda)r^p(\lambda)\mathrm{d}\lambda, \tag{1}$$

where Ω denotes the range of the visible spectrum. We note that Eq. (1) assumes linear behavior of the camera, i.e., that the response V_k^p is proportional to the amount of light entering the camera. For cameras that do not have such a linear response, their RGB responses should be corrected by use of the inverse optoelectronic conversion function.[10,11] Equation (1) can be represented in more-compact notation as

$$\mathbf{V}^p = \mathbf{SLr}^p, \tag{2}$$

where $\mathbf{V}^p$ is the 3×1 vector of V_k^p, $\mathbf{S}$ is the $3 \times N$ matrix of $S_k(\lambda)$, $\mathbf{L}$ is the $N \times N$ diagonal matrix $\mathrm{diag}[L(\lambda_1), L(\lambda_2), \ldots, L(\lambda_N)]$, and $\mathbf{r}^p$ is the $N \times 1$ vector of $r^p(\lambda)$.

According to the dichromatic reflection model[4] and the neutral interface reflection model,[12] reflectance $\mathbf{r}^p$ can be decomposed into body reflectance $\mathbf{r}_B$ and constant surface reflectance $\mathbf{r}_S$, weighted by geometric coefficients α^p and β^p:

$$\mathbf{r}^p = \alpha^p\mathbf{r}_B + \beta^p\mathbf{r}_s + \varepsilon^p, \tag{3}$$

where ε^p is an approximation error in spectral reflectance space.[6] According to our previous study,[6] ε^p is small and therefore Eq. (3) is accurate for color modeling. Substituting Eq. (3) into Eq. (2) yields

$$\begin{aligned}\mathbf{V}^p &= \alpha^p(\mathbf{SLr}_B) + \beta^p(\mathbf{SLr}_S) + \mathbf{SL}\varepsilon^p \\ &= \alpha^p\mathbf{V}_B + \beta^p\mathbf{V}_S + \mathbf{e}^p,\end{aligned} \tag{4}$$

where $\mathbf{e}^p$ is residual error in RGB space and $\mathbf{V}_B$ and $\mathbf{V}_S$ are body and surface colors, respectively. We should note that $\mathbf{V}_B$ is the inherent characteristic of the object surface, whereas $\mathbf{V}_S$ is of the same color as the illuminant, in accordance with the neutral interface reflection model.

3. Algorithm of Color Transfer between Three-Dimensional Objects

A. Calculation of Implicit Geometric Coefficients

In this study, one of our objectives is to substitute body color $\mathbf{V}_B$ into Eq. (4) such that the appearance of a new object can be synthesized. Obviously, coefficients α^p and β^p should be accurately solved before the color synthesis is made. The most straightforward method for solving coefficients α^p and β^p is to employ the ordinary least-squares (LS) method[13] to minimize the error term

$$J = (\mathbf{e}^p)^T\mathbf{e}^p. \tag{5}$$

Let $\mathbf{M} = [\mathbf{V}_B\mathbf{V}_S]$ and $\mathbf{c}^p = [\alpha^p\beta^p]^T$, with T denoting the transpose; coefficient $\mathbf{c}^p$ can be calculated as

$$\mathbf{c}^p = \mathbf{M}^+\mathbf{V}^p, \tag{6}$$

where $\mathbf{M}^+$ is the pseudoinverse of $\mathbf{M}$.

Obviously, the geometric coefficient calculated according to Eq. (6) is optimal in the LS sense for body color $\mathbf{V}_B$. However, as target body color $\mathbf{U}_B$ in the synthesis process is usually different from $\mathbf{V}_B$, the solved coefficient will not be optimal for $\mathbf{U}_B$. In what follows, we analyze the error propagation by considering the color synthesis with target color $\mathbf{U}_B$.

Without loss of generality, we consider only the pixels without surface reflection, i.e., $\beta^p = 0$. Color vectors $\mathbf{U}_B$ and $\mathbf{V}_B$ can be related by use of a 3×1 ratio vector $\boldsymbol{\rho}$ whose kth element is defined as

$$\rho_k = U_{B,k}/V_{B,k}. \tag{7}$$

The equation for synthesized color $\mathbf{U}^p$ that uses target body color $\mathbf{U}_B$ is similar to Eq. (4):

$$\mathbf{U}^p = \alpha^p\mathbf{U}_B + \mathbf{f}^p, \tag{8}$$

where $\mathbf{f}^p$ is synthesis error. For convenience, we further define an operator $\otimes$, namely, vector multiplication, between two 3×1 column vectors, $\mathbf{a} = [a_1\ a_2\ a_3]^T$ and $\mathbf{b} = [b_1\ b_2\ b_3]^T$:

$$\mathbf{a} \otimes \mathbf{b} = [a_1b_1\ a_2b_2\ a_3b_3]^T. \tag{9}$$

Then $\mathbf{U}_B$ can be represented as

$$\mathbf{U}_B = \boldsymbol{\rho} \otimes \mathbf{V}_B. \tag{10}$$

Substituting Eq. (10) into Eq. (8), we get

$$\mathbf{U}^p = \alpha^p(\boldsymbol{\rho} \otimes \mathbf{V}_B) + \mathbf{f}^p \tag{11}$$

Rearranging the terms yields synthesis error $\mathbf{f}^p$, given by

$$\mathbf{f}^p = (\mathbf{U}^p - \boldsymbol{\rho} \otimes \mathbf{V}^p) + \boldsymbol{\rho} \otimes \mathbf{e}^p. \tag{12}$$

From Eq. (12) it is difficult to quantify the error accurately because the actual value of $\mathbf{U}^p$ remains unknown. However, for the second term on the right-hand side, the error propagation is directly related to ratio $\boldsymbol{\rho}$. Therefore it is quite possible that a large error will occur when we synthesize colors with small element values in $\mathbf{V}_B$ with large corresponding element values in $\mathbf{U}_B$.

To deal with this problem, an obvious and simple technique is to give more weight to the channel with larger ρ_k. We define a simple diagonal weighting matrix:

$$\mathbf{w} = \begin{bmatrix} \rho_1 & 0 & 0 \\ 0 & \rho_2 & 0 \\ 0 & 0 & \rho_3 \end{bmatrix}. \tag{13}$$

From the left we multiply each term of Eq. (4) by $\mathbf{w}$; each channel is differently weighted. Therefore the calculation of geometric coefficients α^p and β^p becomes a weighted least-squares (WLS) method,[13] which minimizes the error term

$$J = (\mathbf{we}^p)^T(\mathbf{we}^p) = (\mathbf{e}^p)^T(\mathbf{w}^T\mathbf{w})\mathbf{e}^p, \tag{14}$$

and the geometric coefficient can be solved as

$$\mathbf{c}^p = (\mathbf{wM})^+(\mathbf{wV}^p). \tag{15}$$

B. Calculation of Body Color

In this study we assume that illumination color $\mathbf{V}_S$ is known and thus that one purpose of color transfer between 3-D objects is to recover body color $\mathbf{V}_B$ accurately from images. Tominaga and Wandell employed the singular-value-decomposition technique to calculate the illuminant color from images consisting of two different objects.[14] Tan and Ikeuchi proposed a technique to separate body and surface reflection components from textured surfaces.[15] In this study, as the illumination color is known, we propose a robust technique for estimating body color based on the high correlation between channels. From Eq. (4) it is obvious that the closer coefficient β^p is to zero, the closer $\mathbf{V}^p$ is to $\mathbf{V}_B$, or, equivalently, the farther $\mathbf{V}^p$ is from $\mathbf{V}_S$. We calculate the cosine of including angle θ^p between $\mathbf{V}^p$ and $\mathbf{V}_S$:

$$\cos(\theta^p) = \frac{(\mathbf{V}^p)^T\mathbf{V}_S}{\|\mathbf{V}^p\|\,\|\mathbf{V}_S\|}. \tag{16}$$

We select a collection $\Re_B$ of pixels with small $\cos(\theta^p)$ values (that is, large θ^p), whose surface reflection can be assumed to be quite small. We note that the number of pixels in collection $\Re_B$ is not crucial to the algorithm, as an image always contains adequate numbers of pixels (more than 50%) with mainly diffuse colors. Considering the noise in the imaging process, we believe that 10–20% of the pixels should be appropriate for calculation of body color. The distribution relationship of camera responses between green and red channels of a red plastic cup in $\Re_B$ is shown in Fig. 1. It is obvious that the point cloud forms a straight line with a high correlations coefficient. Let η_{ij} be the slope between the ith and jth channels, which can be calculated as

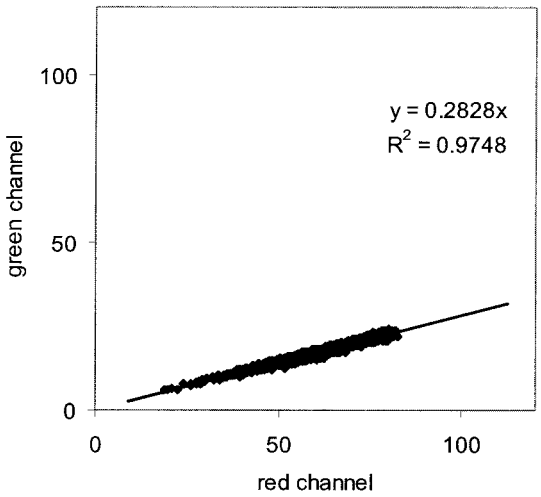

Fig. 1. Distribution of pixel values of the green channel with respect to those of the red channel in color set $\Re_B$.

$$\eta_{ij} = [V_i^p][V_j^p]^+, \tag{17}$$

where the responses V_i^p and V_j^p in set $\Re_B$ are stacked to form row vectors; then the component of body color can be related by the following two equations:

$$V_{B,2} = \eta_{21}V_{B,1}, \tag{18}$$

$$V_{B,3} = \eta_{31}V_{B,1}. \tag{19}$$

Because there are many pixels lying on the fitted straight line (Fig. 1), we can identify $\mathbf{V}_B$ only up to its chromaticity. We add the constraint that

$$\sum_{k=1}^{3} V_{B,k} = 1, \tag{20}$$

and then the chromaticity of body color $\mathbf{V}_B$ can easily be solved from Eqs. (18)–(20):

$$\mathbf{V}_B = \frac{1}{1 + \eta_{21} + \eta_{31}} \begin{bmatrix} 1 \\ \eta_{21} \\ \eta_{31} \end{bmatrix}. \tag{21}$$

We should note that Eq. (21) does not decide the magnitude of body color. For the purpose of color synthesis we choose the color with the largest α^p value with respect to the solved $\mathbf{V}_B$ as the most diffuse reference color $\mathbf{V}_{\mathrm{BR}}$. As the value of β^p is not considered, the chromaticity of $\mathbf{V}_{\mathrm{BR}}$ may not be exactly the same as that of the solved $\mathbf{V}_B$. However, as $\mathbf{V}_{\mathrm{BR}}$ is chosen from set $\Re_B$, we consider that surface reflec-

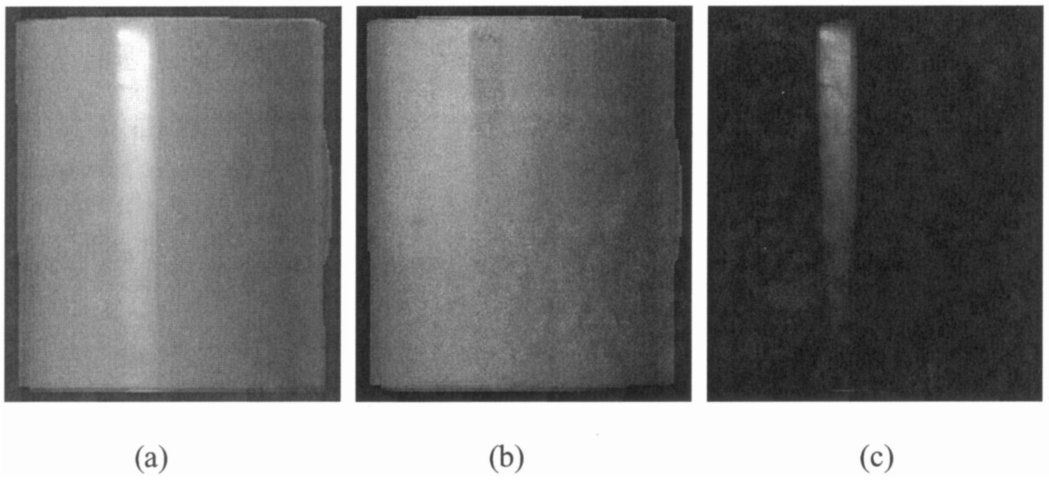

Fig. 2. Results of calculation of pixelwise geometric coefficient (b) α values and (c) β values from color image (a). The coefficients have been rescaled for display.

tion component of $\mathbf{V}_{BR}$ is also quite small, and therefore it can be used to represent the actual diffuse color.

C. Transform between Different Illuminants

For different illuminants it is necessary to predict the new body color. This problem falls into the research area of color constancy.[16,17] The aim of color constancy is to find a linear transform from color vector $\mathbf{V}$ under one illuminant to color vector $\mathbf{V}'$ under another illuminant[17]

$$\mathbf{V}' = \mathbf{T}_L\mathbf{V}, \tag{22}$$

where $\mathbf{T}_L$ is a 3×3 illuminant transform matrix. To solve $\mathbf{T}_L$, three or more distinct training colors can be used. With the calculated $\mathbf{T}_L$, the new body colors under the new illuminant can easily be calculated

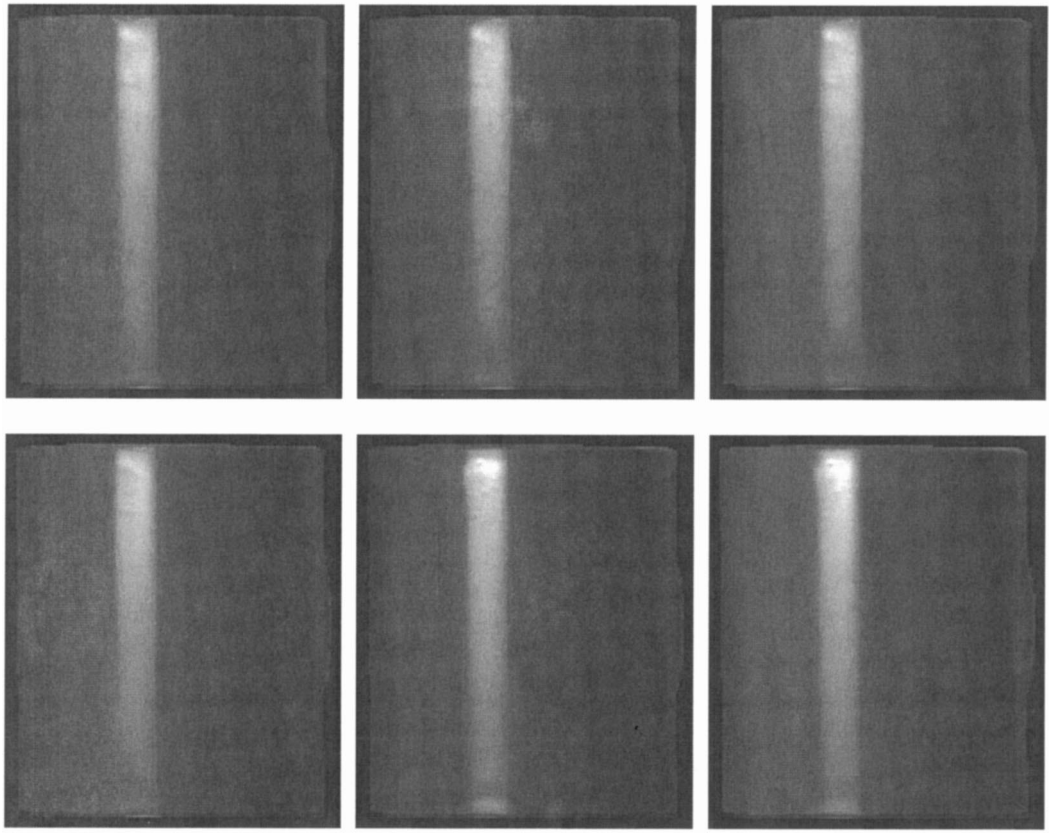

Fig. 3. Top row, red, green, and blue plastic cups synthesized by use of geometric coefficients from a yellow cup and, bottom row, their corresponding target images.

according to Eq. (22). As the surface color is the same as that of the illuminant, it can be obtained directly by imaging of a perfect white diffuser, such as a barium sulfate–coated white reference tile.

D. Segmentation of Multicolored Regions

The discussion above deals only with single-colored objects. For multicolored objects, however, different regions should be separated before color transfer. Many methods have been proposed for the segmentation of 3-D objects when there are highlights and shading. Klinker *et al.* introduced an image segmentation method by generating and verifying a hypothesis about the scene from image data.[18] Gevers and Stokman proposed sophisticated segmentation methods for use with video and multispectral images based on camera noise analysis.[19,20] In this study we propose a simple yet practical segmentation algorithm based on the analysis of fitting error of the dichromatic model, which is described as follows:

First, one seed pixel for each region is manually selected from pixels with mainly body reflection, that is, with medium intensity and saturation. Let $\mathbf{Q}_i$ ($i = 1. . .M$, where M is the number of regions) be the color of the seed pixel for the ith object and $\mathbf{M}_i = [\mathbf{Q}_i\ \mathbf{V}_S]$; we can then calculate the fitting error of the dichromatic reflection model with respect to each seed pixel:

$$E_i^p = \max\left|\mathbf{V}^p - \mathbf{M}_i(\mathbf{M}_i^{+}\mathbf{V}^p)\right|. \tag{23}$$

The right-hand side of Eq. (23) yields the maximum element value of the absolute fitting error. Then label L^p of pixel p can be initially decided according to

$$L^p = \begin{cases} -1 & \min\limits_{i=1\ldots M}(E_i^p) > T \\ \arg\min\limits_{i=1\ldots M}(E_i^p) & \text{otherwise} \end{cases}. \tag{24}$$

After the investigation of a large number of images, we consider that threshold $T = 2.0$ is appropriate in this study. We note that pixels with mainly body reflection will be labeled in this initial stage, as their fitting errors are usually quite small, whereas the large fitting errors often occur in the boundaries of different regions. Hue H^p of pixel p can be calculated as

$$H^p = \arctan\left[\frac{\sqrt{3}(V_2^p - V_1^p)}{2V_3^p - V_1^p - V_2^p}\right]. \tag{25}$$

In an ideal case, according to the dichromatic reflection model the value of H^p should be constant for each single-colored object. In practice, however, because of imaging noises we regard the statistical distribution of hue as a normal distribution. Let μ_i and σ_i be the mean and the standard deviation, respectively, of the ith object calculated from the initial segmentation step; the probability that H^p belongs to the ith object can be decided according to the normal distribution as

$$\text{prob}(i\,|\,H^p) = \frac{1}{\sqrt{2\pi}\sigma_i}\exp\left[-\frac{(H^p - \mu_i)^2}{2{\sigma_i}^2}\right]. \tag{26}$$

Thus the initially unassigned L^p can be decided according to Bayes decision theory[21]:

$$L^p = \arg\max_{i=1\ldots M}[\text{prob}(i\,|\,H^p)]. \tag{27}$$

Table 1. Mean Color Difference ΔE_{94}* of Color Transfer between Cups of Different Colors by the LS and WLS Methods[a]

		Target Cups			
Source Cup	Method	Red	Green	Blue	Yellow
Red	LS	0.441	1.634	1.716	2.844
	WLS	0.482	1.542	1.688	2.854
Green	LS	**2.412**	1.240	1.255	**4.543**
	WLS	**2.061**	1.240	1.278	**4.073**
Blue	LS	**2.482**	1.190	0.341	**5.332**
	WLS	**1.441**	1.388	0.340	**3.328**
Yellow	LS	0.814	1.644	1.607	1.833
	WLS	0.755	1.648	1.710	1.833

[a]The values set in boldface type indicate significant improvement of WLS. The reference colors were selected at the same pixel positions, which were (75, 23, 28), (16, 40, 47), (41, 36, 64), and (123, 87, 27) for the red, green, blue, and yellow cups, respectively.

4. Experiment and Discussion

Based on the discussion above, we summarize the steps in image-based color appearance transfer between 3-D objects as follows:

(1) Separate the multicolored regions if necessary.
(2) Calculate the diffuse colors of different regions for color transfer.
(3) Recover the geometric coefficient by using the WLS technique.
(4) Calculate the new body and surface colors under a new illuminant if necessary.
(5) Perform color synthesis for 3-D objects.

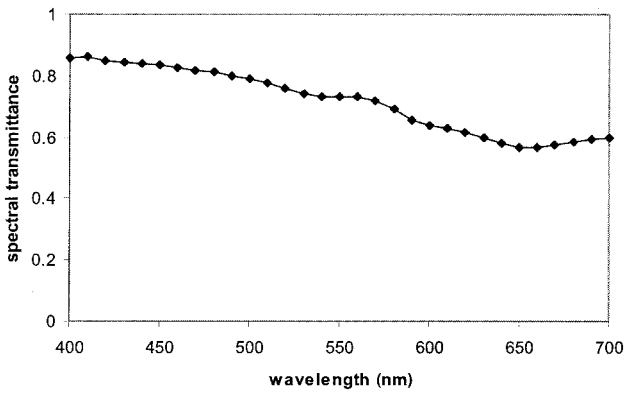

Fig. 4. Spectral transmittance of the blue filter that was used to produce a new illuminant.

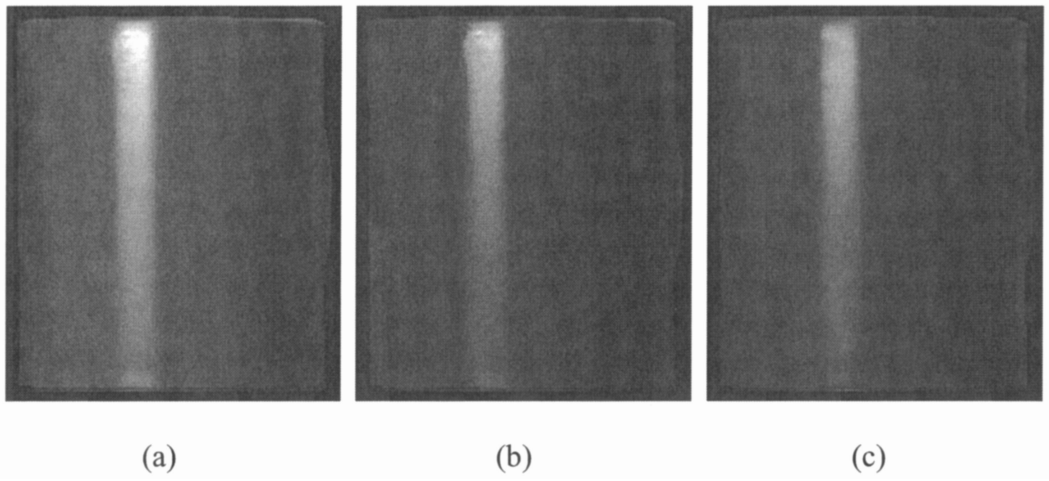

Fig. 5. Results of synthesis under a different illuminant: (a) original blue image, (b) synthesized red image under the new illuminant, (c) actual red image acquired under the new illuminant.

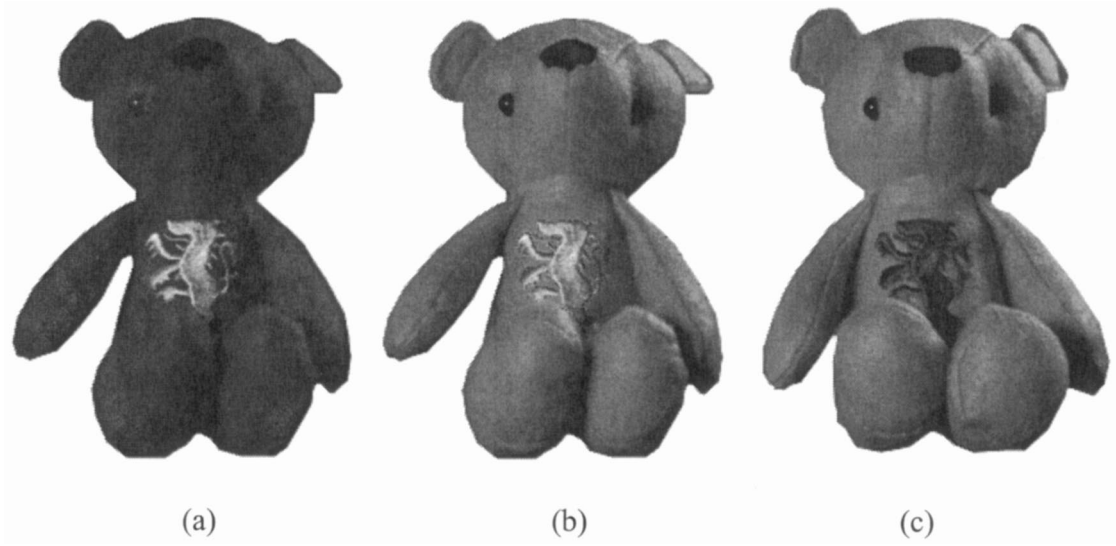

Fig. 6. Experimental results of the color transfer method. (b) The synthesized image (yellow body) was produced by use of (a) the geometric information of the original image (red body) and (c) the yellow body color of the target image.

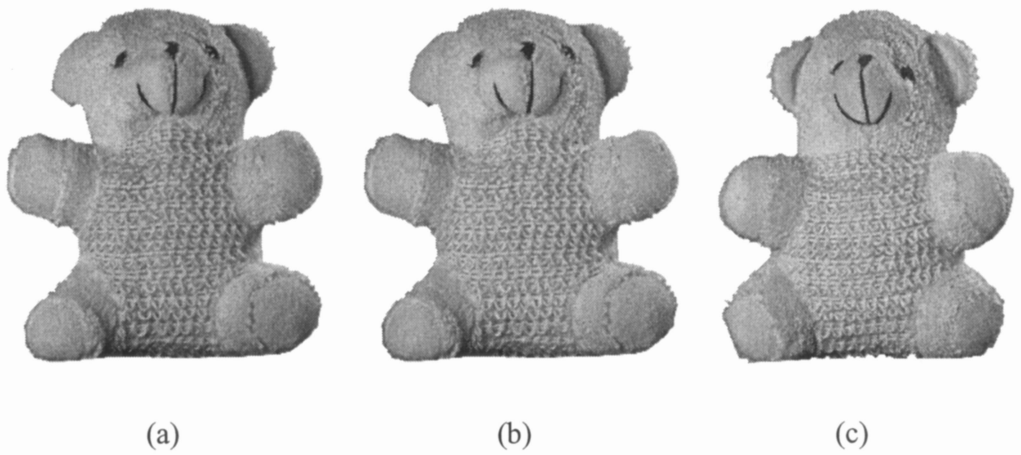

Fig. 7. Experimental results of the color transfer method. (b) The synthesized image (blue body) was produced by use of (a) the geometric information of the original image (pink body) and (c) the blue body color of the target image.

In the experiment we used a QImaging Retiga EXi digital 12-bit monochromatic CCD camera together with a QImaging RGB liquid-crystal color filter to acquire RGB color images. To investigate the linearity of the camera, we set up the imaging system according to the IEC standard[11] and measured the luminance of each gray-scale patch, using a spectroradiometer (Photo Research Model PR704), and acquired the corresponding RGB responses of the camera. The very high correlation ($R^2 = 0.999$) between luminance and RGB responses indicated that the linearity of the camera is very good and thus that no further linearization is needed. We obtained the illuminant color by imaging a perfect white patch (a barium sulfate-coated white reference tile). In this study the images were viewed on a Sony Trinitron monitor screen. The monitor was characterized by use of the well-known gain-offset-gamma model.[22] We used four plastic cups with the same shape but different colors to investigate the accuracy of the recovered geometric coefficient. Figure 2 shows the result of recovery of geometric coefficient α and β of the yellow cup. As expected, the variation of body reflection is quite smooth, whereas that of surface reflection is abrupt. Figure 3 shows the images synthesized with the recovered α and β of the yellow cup and the body colors of the corresponding target images. Because of the different coating effects and glossiness of individual cups, the colors in a highlighted region may differ from one another. Despite the difference in highlight regions, we found that the color appearances of each pair of synthesized and target images were perceptually close. To quantify the error in color synthesis, first we convert the RGB space of images into the display CIELAB space according to the gain-offset-gamma model of the monitor,[22] and then calculate the mean CIE 1994 color difference ΔE_{94}^* (not including the pixels in highlight regions) between synthesized and target images by using any two images as source and target. We use the ΔE_{94}^* value instead of the RGB error because the former is perceptually close to human perception. The ΔE_{94}^* values when LS and WLS methods are used are given in Table 1. As expected, when the corresponding element value is large in the target image while it is small in the source image, the improvement of WLS is significant (bold face numbers). For other cases, the color differences of LS and WLS are similar. Both Fig. 3 and Table 1 show that the performance of the proposed algorithm is quite good.

A light-blue filter was used in front of the lens of the camera to produce a new illuminant condition. The spectral transmittance of this filter is given in Fig. 4. We prefer to use the filter instead of replacing the illuminant; thus we can keep the spatial distribution of the illuminant unchanged. Illuminant transform matrix $\mathbf{T}_L$ was calculated by use of the 24 color patches of the Macbeth ColorChecker and is given as follows:

Fig. 8. Two examples of colorization with user-specified target colors. Top left, yellow body, red shirt, blue horn; top right, purple body, blue shirt, yellow horn; bottom left, blue background; bottom right, yellow background.

$$\mathbf{T}_L = \begin{bmatrix} 0.623 & 0.027 & -0.003 \\ -0.006 & 0.745 & 0.013 \\ 0.002 & -0.007 & 0.840 \end{bmatrix}. \quad (28)$$

The mean color difference ΔE_{94}^* between the actual color and the color calculated from $\mathbf{T}_L$ is 0.385. The color synthesis under the new illuminant is as shown in Fig. 5. It can be seen that the color appearances of the two images are quite close. The results for multicolored objects are shown in Figs. 6 and 7. Despite the different positions of the synthesized and the target objects, their colors appear quite similar. Note that, in the segmentation algorithm, only fitting error and hue distribution were considered. As a result, the algorithm may be unsuccessful in producing segmentation when the colors of two regions are similar. In this case a more-sophisticated segmentation method can be applied. Nevertheless, from all the experimental results, the whole effect of color appearance transfer between 3-D objects is promising. For practical applications, we can also modify the color appearance of objects by direct specification of target colors, as shown in Fig. 8. It can be found that the synthesized images seem realistic and that the highlight and shadow areas are well preserved.

5. Conclusions

In this study method by which the appearance of a color can be transferred between 3-D objects in two-dimensional images has been proposed. The method includes the following elements: First, the camera's response is modeled according to a dichromatic reflection model, i.e., a linear combination of body and

surface reflection. Second, the geometric coefficient is calculated by the WLS technique; the error propagation during color synthesis is taken into account. Third, we assume that the color of the illuminant is known, and then the body color is calculated. Pixels with little surface reflection are selected according to the angle between pixel color and illuminant color. The chromaticity of the body color is then calculated according to the degree of correlation between different channels. Fourth, the illuminant's transform matrix is calculated such that color synthesis can be applied for a new illuminant. Finally, a dichromatic-based segmentation technique is proposed for images that consist of multicolored regions.

The experimental results have shown that the color accuracy is quite high. The error in color reproduction in RGB space is small, and the appearance of the synthesized color is quite natural. The algorithm can be used in image-based design and visualization of virtual color 3-D objects.

We thank the anonymous reviewers for their comments, which substantially improved this paper. This research was supported by the Hong Kong Polytechnic University.

References

1. E. Reinhard, M. Ashikhmin, B. Gooch, and P. Shirley, "Color transfer between images," IEEE Comput. Graph. Appl. **21,** 34–41 (2001).
2. T. Welsh, M. Ashikhmin, and K. Mueller, "Transferring color to grayscale images," ACM Trans. Graphics **20,** 277–280 (2002).
3. A. Levin, D. Lischinski, and Y. Weiss, "Colorization using optimization," ACM Trans. Graphics **23,** 689–694 (2004).
4. S. A. Shafer, "Using color to separate reflection components," Color Res. Appl. **10,** 210–218 (1985).
5. L. Liu and G. Xu, "Color change method based on dichromatic reflection model," in *Proceedings of the International Conference on Signal Processing* (Institute of Electrical and Electronics Engineers, Piscataway, N.J., 1996), pp. 1246–1249.
6. J. H. Xin and H. L. Shen, "Accurate color synthesis of three-dimensional objects in an image," J. Opt. Soc. Am. A **21,** 713–723 (2004).
7. F. E. Nicodemus, J. C. Richmond, J. J. Hsia, I. W. Ginsberg, and T. Limperis, "Geometric considerations and nomenclature for reflectance," Monograph 160 (National Institute of Standards and Technology, Rockville, Md., 1997).
8. G. J. Ward, "Measuring and modeling anisotropic reflection," ACM Comput. Graphics **26,** 265–272 (1992).
9. G. Sharma and H. J. Trussell, "Digital color imaging," IEEE Trans. Image Process **6,** 901–932 (1997).
10. P. L. Vora, J. E. Farrell, J. D. Tietz, and D. H. Brainard, "Image capture: simulation of sensor responses from hyperspectral images," IEEE Trans. Image Process **10,** 307–316 (2001).
11. International Electrotechnical Commission, "Multimedia systems and equipment - Colour measurement and management. 9. Digital cameras," 2nd ed., Standard IEC 61966-9 (International Electrotechnical Commission, Geneva, Switzerland, 2003).
12. H. C. Lee, E. J. Breneman, and C. P. Schulte, "Modeling light reflection for computer vision," IEEE Trans. Pattern Anal. Mach. Intell. **12,** 402–409 (1990).
13. F. A. Graybill and H. K. Iyer, *Regression Analysis: Concepts and Applications* (Duxbury, Belmont, California, 1994).
14. S. Tominaga and B. A. Wandell, "Standard surface-reflectance model and illuminant estimation," J. Opt. Soc. Am. A **6,** 576–584 (1989).
15. R. T. Tan and K. Ikeuchi, "Separating reflection components of textured surfaces using a single image," in *Proceedings of the Ninth IEEE International Conference on Computer Vision* (Institute of Electrical and Electronics Engineers, Piscataway, N.J., 2003), pp. 870–877.
16. K. Barnard, V. Cardei, and B. Funt, "A comparison of computational color constancy algorithms. I. Methodology and experiments with synthesized data," IEEE Trans. Image Process **11,** 972–983 (2002).
17. G. D. Finlayson, M. S. Drew, and B. V. Funt, "Color constancy: generalized diagonal transforms suffice," J. Opt. Soc. Am. A **11,** 3011–3019 (1994).
18. G. J. Klinker, S. A. Shafer, and T. Kanade, "A physical approach to color image understanding," Int. J. Comput. Vision **4,** 7–38 (1990).
19. T. Gevers and H. Stokman, "Classifying color edges in video into shadow-geometry, highlight, or material transitions," IEEE Trans. Multimedia **5,** 237–243 (2003).
20. T. Gevers and H. M. G. Stokman, "Robust photometric invariant region detection in multispectral images," Int. J. Computer Vision **53,** 135–151 (2003).
21. R. Duda and P. Hart, *Pattern Classification and Scene Analysis* (Wiley, New York, 1973).
22. R. S. Berns, R. J. Motta, and M. E. Gorzynski, "CRT colorimetry. I. Theory and practice," Color Res. Appl. **18,** 299–314 (1993).